Global Journal of Pure and Applied Mathematics (GJPAM) ISSN 0973-1768 Volume 12,Number 4 (2016)

Simulation of two-sided deep cavity flows by lattice Boltzmann Multi-Relaxation-Time Model

D. Arumuga Perumal
Department of Mechanical Engineering,
National Institute of Technology Karnataka,
Surathkal, Mangalore, India – 575 025
Email: perumal@nitk.edu.in

***Abstract*—The present work discusses the characteristics of incompressible viscous flow within a two-sided lid-driven cavity with its two opposite walls moving with a uniform velocity in parallel and antiparallel direction by multi-relaxation-time lattice Boltzmann technique. It is realized that, single-relaxation-time lattice Boltzmann technique have numerous deficiencies. Other than the single-relaxation-time technique, the multi-relaxation-time technique, which has certain points of interest, is additionally utilized. The attributes of the present flow problem are investigated for various Reynolds number furthermore for various aspect ratios. Accurately, the impact of Reynolds number and aspect ratio on the flow pattern and in addition on the strengths of vortices inside the cavity is examined. The Reynolds number effect on the flow structure is virtually manifested with the aid of the streamlines and velocity profiles.**

Keywords*— *lattice Boltzmann technique; single-relaxation-time; multi-relaxation-time; two-dimensional lid-driven cavity; D2Q9 model.

I. INTRODUCTION

In the area of Computational Fluid Dynamics (CFD), two important approaches to simulate fluids have been developed in the last few decades. First, the classical approach is based on the numerical solutions of the Navier-Stokes equations [1]. Alternatively, Navier-Stokes equation in continuum theory can be derived from the Boltzmann equation in the limit of small Knudsen numbers [2]. Recently, the Lattice Boltzmann technique based on Boltzmann equation has emerged as a new and effective numerical approach of CFD and it has achieved considerable success in simulating fluid flows [3]. Numerous extensions in the past few years have made the lattice Boltzmann technique used for a wide range of problems including thermal flows, porous media, magneto-hydrodynamics, vortex dynamics, turbulent flows, multi-phase flows, free-surface flows, fluid-structure interactions, visco-elastic fluids, particulate suspensions and other complex fluids [4].

Many of the LBM works published so far reveals a plethora of issues concerning single-relaxation-time Lattice Boltzmann technique (LBT-SRT) and its applicability to incompressible viscous flows in particular [5]. It is also known that, the simple and popular incompressible SRT-LBM has few shortcomings. In the LBT-SRT model formulation, both the bulk and shear viscosities are determined by the same relaxation time. Mainly, in LBT-SRT model the relaxation time equal to 0.5 is the critical value for ensuring a non-negative kinematic viscosity. Numerical instability can be expected in LBT-SRT model for relaxation time close to this critical value. It is also known that, the LBT-SRT model can be improved in terms of stability, computational efficiency by using Multi-relaxation-time Lattice Boltzmann technique (LBT-MRT) [6].

Lallemand and Luo [7] showed the robustness of the Multi-Relaxation-Time Lattice Boltzmann method (LBT-MRT) and presented high accuracy results and numerical stability of high Reynolds numbers. They have performed the detailed theoretical analysis on the dispersion, dissipation and stability characteristics of a generalized Lattice Boltzmann Equation model proposed by d'Humieres [8]. It is known that, the flow in a cavity driven by the steady motion of a lid is a classical bench mark problem in fluid mechanics [9]. A few researchers have carried out simulations of the single-sided lid-driven cavity flows using LBT-MRT [10]. Detailed study of two-sided lid-driven deep cavity as to how they grow with increasing Reynolds number has not yet been made by LBT-MRT. Therefore, to demonstrate the ability of the lattice Boltzmann equation with multi-relaxation-time model we simulate the two-dimensional cavity problems such as single-sided lid-driven square cavity flow, two-sided lid-driven square cavity flow and two-sided lid-driven rectangular cavity flow.

The organization of the rest of this paper is as follows. In Section 2, Multi-Relaxation-Time Lattice Boltzmann Method is described in some detail. In Section 3 the two-sided lid-driven cavity problem is described and the results with parallel and antiparallel motion of the walls for different aspect ratios are presented in detail. Concluding remarks are made in Section 4.

This paper was presented by the author in the National Conference on *Advances in Mathematics and its Applications to Science and Engineering* (AMASE-2016) conducted in Department of Mathematics, University College of Engineering Pattukkottai, Thanjavur, Tamil Nadu, India, on 22nd January 2016.

II. LBT MULTI-RELAXATION-TIME

Most of the Lattice Boltzmann technique works published concerning with the Lattice Bhatnagar-Gross-Krook (LBGK) model because of its simplicity [2]. Only a few works used LBT-MRT to predict fluid flow parameters. For simulating 2D flows a D2Q9 square lattice model is used and the discrete particle velocities are represented as $\left\{ \boldsymbol{c_i} \middle| i = 0, 1,.....,N \right\}$ and the particle distribution function is represented as $\left\{ f_i(\mathbf{x},t) \middle| \ i = 0, 1,...., N \right\}$. The discretized particle distribution function in a vector space $\underline{R}$ can be written as [10]

$$\left| f_i(\mathbf{x}_i, t_n) \right\rangle = \left\{ f_0(\mathbf{x}_i, t_n),\ f_1(\mathbf{x}_i, t_n), ..., f_N(\mathbf{x}_i, t_n) \right\}^T \quad (1)$$

The Multi-Relaxation-Time Lattice Boltzmann technique (LBT-MRT) evolution equation can be written in discretized form [10]

$$\left| f_i(\mathbf{x}_i + \boldsymbol{c}_i \Delta t, t_n + \Delta t) \right\rangle - \left| f_i(\mathbf{x}_i, t_n) \right\rangle = -M^{-1} \underline{S} \left(\left| m_i(\mathbf{x}_i, t_n) \right\rangle - \left| m_i^{eq}(\mathbf{x}_i, t_n) \right\rangle \right) \quad (2)$$

where $\underline{S}$ is the diagonal matrix, M for the *D2Q9* square lattice model is a 9×9 transformation matrix that linearly transforms the velocity distribution functions f_i to the macroscopic moments. The moments for the two-dimensional *D2Q9* square lattice model are given as $\left| m_i \right\rangle = (\rho, e, \varepsilon, j_x, q_x, j_y, q_y, p_{xx}, p_{xy})^T$. Here ρ is the fluid density, e is the energy, ε is related to square of energy, j_x and j_y are the momentum density (mass flux), q_x and q_y are the energy flux, p_{xx} and p_{xy} correspond to the diagonal and off-diagonal component of the viscous stress tensor. Diagonal matrix ($\underline{S}$) can be written as $\underline{S} = (0, s_2, s_3, 0, s_5, 0, s_7, s_8, s_9)$. It is known that for the LBT-MRT model if we set $s_8 = s_9 = \frac{1}{\tau}$ then we can get same viscosity formula for the LBT-SRT model. In LBT-MRT model it is more flexible to chose the rest of the relaxation parameters such as s_2, s_3, s_5, s_7. In general these parameters can be chosen to be slightly larger than unity. Another important point, is to recover LBT-SRT model results we can set LBT-MRT model parameters such as $s_2, s_3, s_5, s_7, s_8, s_9 = \frac{1}{\tau}$. The transformation matrix M can be written as

$$M = \begin{pmatrix} 1 & 1 & 1 & 1 & 1 & 1 & 1 & 1 & 1 \\ -4 & -1 & 2 & -1 & 2 & -1 & 2 & -1 & 2 \\ 4 & -2 & 1 & -2 & 1 & -2 & 1 & -2 & 1 \\ 0 & 1 & 1 & 0 & -1 & -1 & -1 & 0 & 1 \\ 0 & -2 & 1 & 0 & -1 & 2 & -1 & 0 & 1 \\ 0 & 0 & 1 & 1 & 1 & 0 & -1 & -1 & -1 \\ 0 & 0 & 1 & -2 & 1 & 0 & -1 & 2 & -1 \\ 0 & 1 & 0 & -1 & 0 & 1 & 0 & -1 & 0 \\ 0 & 0 & 1 & 0 & -1 & 0 & 1 & 0 & -1 \end{pmatrix} \quad (3)$$

The present *D2Q9* square lattice model used here has nine discrete particle velocities. Each node of which has eight neighbours connected by eight links and a rest particle at centre as shown in Figure 1. The particle velocities are defined as [11]

$$\begin{aligned} c_i &= 0, \quad i = 0 \\ c_i &= (\cos(\pi/4(i-1)), \sin(\pi/4(i-1))), \quad i = 1, 2, 3, 4 \\ c_i &= \sqrt{2}(\cos(\pi/4(i-1)), \sin(\pi/4(i-1))), \ i = 5, 6, 7, 8. \end{aligned} \quad (4)$$

The macroscopic quantities such as density ρ and momentum density $\rho \boldsymbol{u}$ are defined as velocity moments of the distribution function f_i as follows:

$$\rho = \sum_{i=0}^{N} f_i, \quad (5)$$

$$\rho \boldsymbol{u} = \sum_{i=0}^{N} f_i \boldsymbol{c_i} \quad (6)$$

The density is determined from the particle distribution function. The macroscopic density and the velocities satisfy the Navier-Stokes equations in the low-Mach number limit. This can be demonstrated by using the Chapman-Enskog expansion. In the present nine-speed square lattice model, a suitable equilibrium distribution function that has been proposed is [11]

$$\begin{aligned} f_i^{(0)} &= \rho w_i \left[1 - \frac{3}{2} \boldsymbol{u}^2 \right], \ i = 0 \\ f_i^{(0)} &= \rho w_i \left[1 + 3(\boldsymbol{c_i}.\boldsymbol{u}) + 4.5\ (\boldsymbol{c_i}.\boldsymbol{u})^2 - 1.5\ \boldsymbol{u}^2 \right], \ i = 1, 2, 3, 4 \\ f_i^{(0)} &= \rho w_i \left[1 + 3(\boldsymbol{c_i}.\boldsymbol{u}) + 4.5\ (\boldsymbol{c_i}.\boldsymbol{u})^2 - 1.5\ \boldsymbol{u}^2 \right], \ i = 5, 6, 7, 8 \end{aligned} \quad (7)$$

where the lattice weights are given by $w_0 = 4/9,\ w_1 = w_2 = w_3 = w_4 = 1/9$ and $w_5 = w_6 = w_7 = w_8 = 1/36$. The relaxation time is related to the viscosity by [11]

$$\tau = \frac{6\upsilon + 1}{2} \quad (8)$$

where υ is the kinematic viscosity measured in lattice units. The implementation of the boundary condition for the LBT-MRT model is the same as the LBT-MRT. At a boundary point, the particle distribution functions along all inward directions are determined by the bounce-back rule. To ensure the no-slip boundary condition ($\boldsymbol{U} = 0$) on the wall, Yu *et al.* [3] suggested a improved bounce-back boundary condition using a linear interpolation formula

$$f_{\tilde{i}}(\mathbf{x}_w) = f_{\tilde{i}}(\mathbf{x}_w) + \frac{\Delta}{1+\Delta}\left(f_{\tilde{i}}(\mathbf{x}_f + \boldsymbol{c}_i) - f_{\tilde{i}}(\mathbf{x}_w) \right) \quad (9)$$

The above boundary condition is valid for both $\Delta < 0.5$ and $\Delta \geq 0.5$. For a moving wall they added additional momentum [3]

$$f_{\tilde{i}}(\mathbf{x}_W, t+\Delta t) = f_i(\mathbf{x}_\mathbf{W}, t+\Delta t) + 2w_i\rho\frac{3}{c^2}\boldsymbol{c_i}.\boldsymbol{u}_\mathbf{W} \quad (10)$$

where $f_{\tilde{i}}$ indicates post-collision state. For the moving wall, uniform plate velocity $\boldsymbol{U}$ = 0.1, considering the validity of using Lattice Boltzmann technique in simulating incompressible flows. The LBT-MRT is solved in the solution domain subjected to the above initial and boundary conditions on a uniform two-dimensional lattice structure.

A. Code Validation

In order to validate the developed 2D incompressible viscous flow algorithm, the present LBT-MRT code is first applied to the single-sided lid-driven square cavity flow problem. The configuration of single-sided lid-driven cavity flow considered here consists of a two-dimensional square cavity whose top plate moves from left to right with constant velocity U = 0.1, while the other three cavity wall boundaries are fixed. The present simple geometry makes ideal to study and analyze the behaviour of vortices in closed boundary domains. It is known that, the fundamental characteristics of the single-sided lid-driven cavity flow are the emergence of a large primary vortex in the centre of a cavity and of secondary vortices in the lower two bottom cavity corners. The Reynolds number is defined $Re = UL/\nu$ where L is the height or width of the cavity and ν is the kinematic viscosity. In the present work, the lattice size of 181 x 181 is used for Re = 1000. Figure 2 depicts the streamline pattern at Re = 1000 obtained through LBM-MRT code, which closely resembles those given by other researchers [2, 9, 10, 11]. Particularly, an excellent agreement can be found between the present LBT-MRT model and the benchmark results of Ghia *et al.* [12].

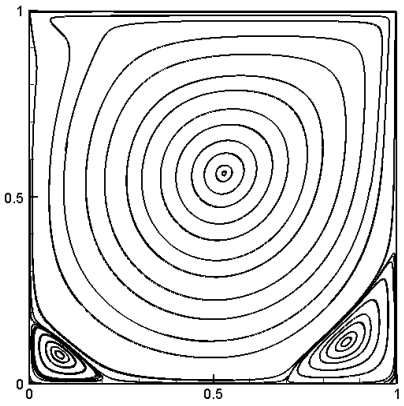

Figure 2: Streamline pattern for the single-sided square cavity flow for Re = 1000.

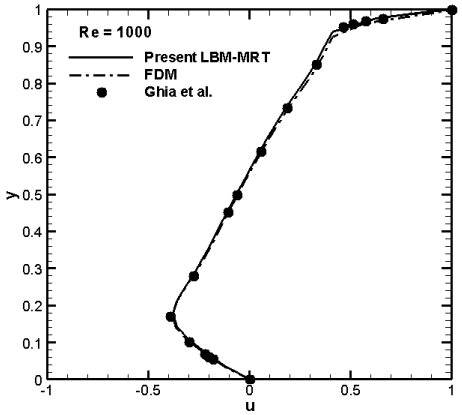

(a)

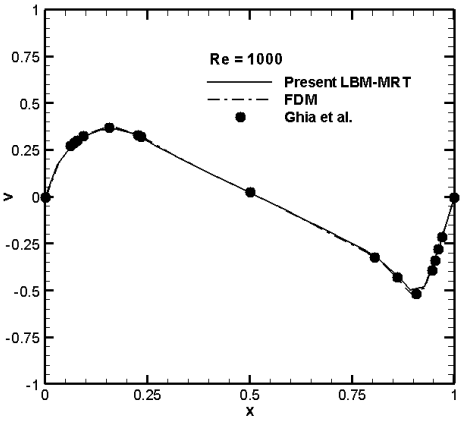

(b)

Figure 3: Code validation: (a) *u*-velocity along vertical centreline and (b) *v*-velocity along horizontal centreline for single-sided lid-driven square-cavity (Re = 1000).

Figure 3(a) shows the *u*-velocity distribution along the vertical centreline, 3(b) shows the *v*-velocity distribution along the horizontal centreline, compared with Ghia's results [12] and FDM results [1]. It can be seen that the present LBM-MRT model result agrees very well with existing results of Ghia *et al.* [12] and Perumal & Dass [11]. The present results conclude that the present LBT-MRT model can be extended to two-dimensional two-sided incompressible viscous flow without increasing computational efficiency.

III. TWO-SIDED LID-DRIVEN CAVITY FLOW

The classical single-sided lid-driven cavity problem has been extended to two-sided lid-driven cavity problem by two facing walls moving in the same (or) opposite directions [1]. In the parallel wall motion we consider, both the upper and lower facing walls moving from left to right in the *x* direction with the same velocity of $\boldsymbol{U}$ = 0.1. In the antiparallel wall motion the lower and upper facing walls moving in opposite directions along the *x*-axis with the same velocity of $\boldsymbol{U}$ = 0.1. All the results presented in the paper are independent of the lattice size and they are substantiated carefully. The boundary conditions for the parallel and antiparallel wall motion are shown in Figures 4 (a) and (b).

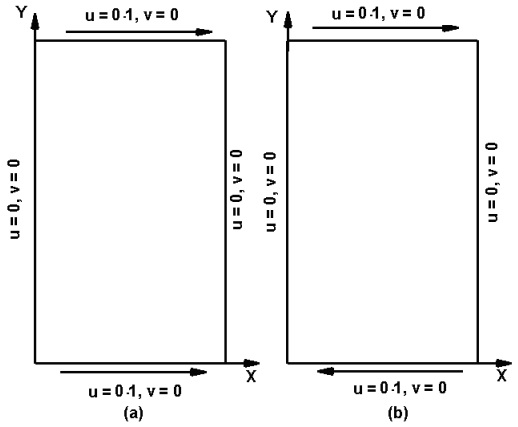

Figure 4: Two-sided lid-driven cavity for (a) parallel wall motion (b) antiparallel wall motion with boundary conditions.

B. Parallel Wall Motion

C. Square Cavity Flow

In the present section, the two-sided lid-driven square cavity for the case of upper and lower facing walls moving in same direction along the *x*-axis with Reynolds number increasing from *Re* = 10 to 1500 using LBT-MRT model on a 161×161 lattice arrangement is studied. Figure 5 shows the streamlines are symmetrical with respect to a line parallel to facing walls and passing through the cavity centre for all Reynolds numbers.

At *Re* = 10, it is observed that a pair of primary re-circulating vortices formed at the lower and upper cavities and form a free shear layer in between. At *Re* = 500, besides the pair of primary vortices, a pair of smaller counter-rotating vortices symmetrically placed about the horizontal centreline near the centre of the right cavity wall. It is also observed that, with the increase in Reynolds number (*Re* = 1500) the primary vortex cores moves towards the centres of the top and bottom halves of the lid-driven cavities and these pair of secondary vortices grow in size.

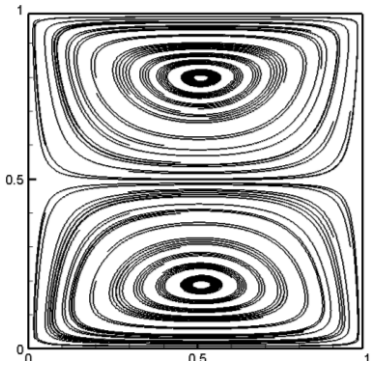

(a) *Re* = 10

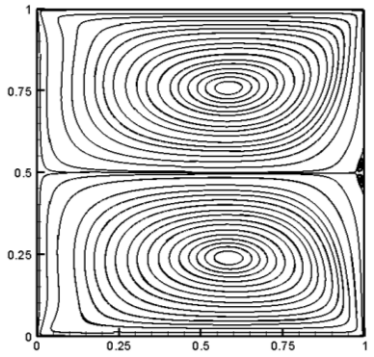

(b) *Re* = 500

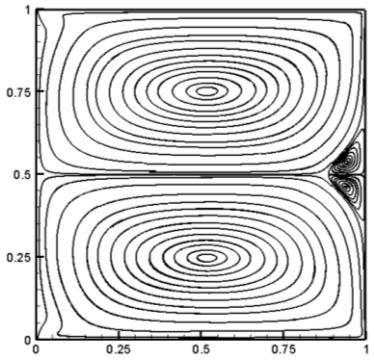

(c) *Re* = 1500

Figure 5: Streamline patterns of double-sided square cavity with parallel wall motion for different Reynolds numbers.

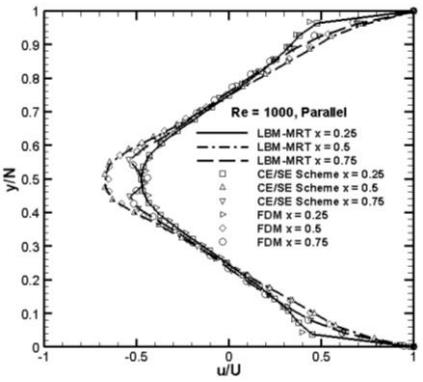

(a)

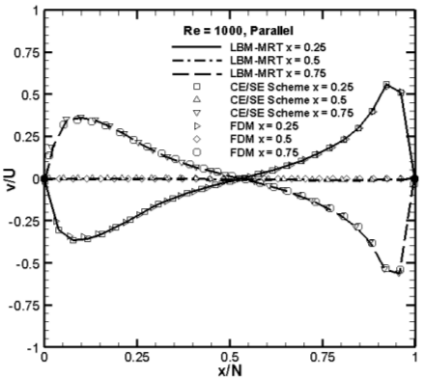

(b)

Figure 6: Parallel wall motion, *Re* = 1000: (a) horizontal velocity *u* along vertical lines (b) vertical velocity *v* along horizontal lines passing through *y* = 0.25, 0.50 and 0.75.

Figures 6 shows the comparison of horizontal velocity profiles along vertical lines and vertical velocity profiles along horizontal lines passing through different points of the two-sided lid-driven square cavity (parallel wall motion) for various Reynolds numbers. Agreement of the velocity profiles given by present LBT-MRT model with those given by the FDM [1] and CE/SE Scheme [13] is excellent. All these results show that the agreement is very good, which further substantiates the accuracy of the present LBT-MRT computations.

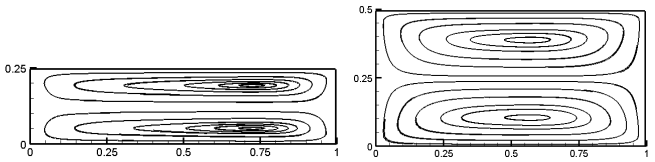

(a) *K* = 0.25 (b) *K* = 0.50

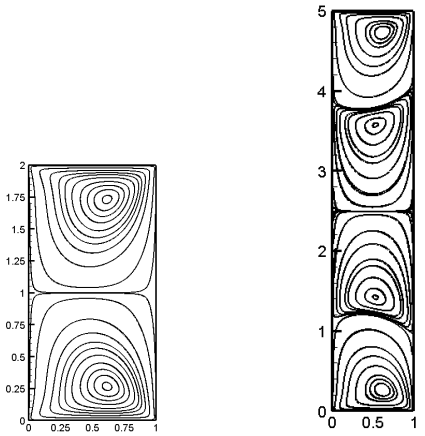

(c) *K* = 2.0 (d) *K* = 5.0

Figure 7: Streamline patterns of *Re* = 10 for double-sided parallel wall motion with different Aspect ratios (a) *K* = 0.25, (b) *K* = 0.50, (c) *K* = 2.0 and (d) *K* = 5.0.

D. Aspect Ratio Effect

To study the aspect ratio effect, low to high aspect ratios of *K* = 0.25, 0.5, 2.0 and 5.0 is considered. It is known that, both walls move in same direction, it can generate their own primary vortex. As aspect ratio *K* increases from 0.25 to 5.0, a sequence of streamline patterns is obtained for Reynolds numbers *Re* = 10, 500 and 1500 as shown in Figures 7-9. Figures 7 (a), (b), (c) and (d) respectively show the streamline patterns of *Re* = 10 where the aspect ratios *K* = 0.25, 0.5, 2.0 and 5.0. At low Reynolds number *Re* = 10 for different aspect ratios *K* the following observations are made. It is seen that, at all aspect ratios the streamlines are symmetrical with respect to a line parallel to facing walls and passing through the cavity centre.

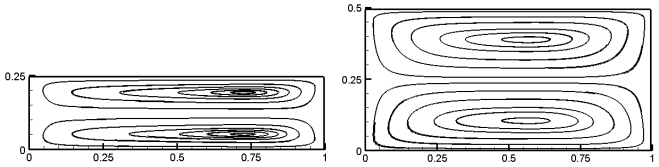

(a) *K* = 0.25 (b) *K* = 0.50

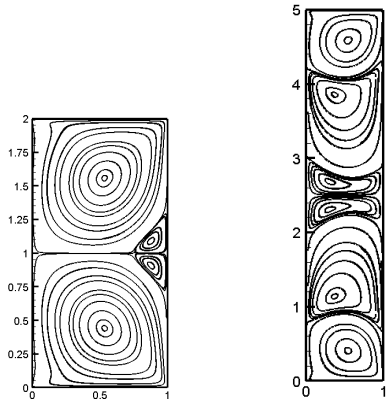

(c) *K* = 2.0 (d) *K* = 5.0

Figure 8: Streamline patterns of *Re* = 500 for double-sided parallel wall motion with different Aspect ratios (a) *K* = 0.25, (b) *K* = 0.50, (c) *K* = 2.0 and (d) *K* = 5.0.

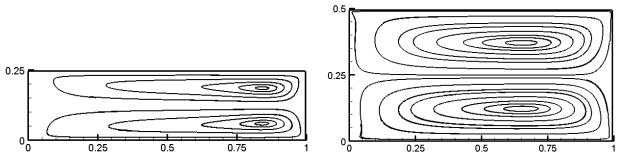

(a) *K* = 0.25 (b) *K* = 0.50

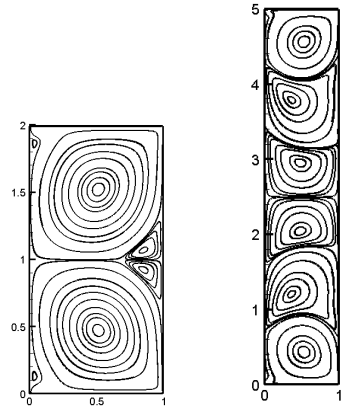

(c) *K* = 2.0 (d) *K* = 5.0

Figure 9: Streamline patterns of *Re* = 1500 for double-sided parallel wall motion with different Aspect ratios (a) *K* = 0.25, (b) *K* = 0.50, (c) *K* = 2.0 and (d) *K* = 5.0.

At *K* = 0.25, two primary vortices appear in the right corner of the cavity. With the increase of aspect ratio from 0.25, the primary vortices centre shifts from the top-right corner towards the geometric centre of the cavity. At high aspect ratio of *K* = 5.0, four primary vortices are generated due to motion of upper and lower facing walls. Figure 8 depicts the moderate Reynolds number of *Re* = 500 for different aspect ratios. Figure 9 depicts the high Reynolds number of *Re* = 1500 for different aspect ratios. As aspect ratio increases the vortices strength also increases.

E. Antiparallel Wall Motion

F. Square Cavity Flow

The streamline patterns for the two-sided lid-driven square cavity for the case of upper and lower facing walls move in the opposite direction with Reynolds number increasing from *Re* = 10 to 1500 using LBT-MRT model on a 161×161 lattice arrangement are shown in Figure 10. From the Figures it is observed that, a single primary vortex centred at the geometric centre of the cavity is formed at low Reynolds numbers. The streamline patterns for *Re* = 1500 are shown in Figures 10(c).

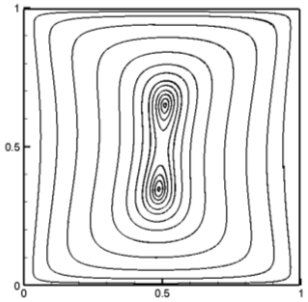

(a) *Re* = 10

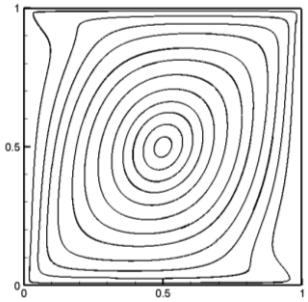

(b) *Re* = 500

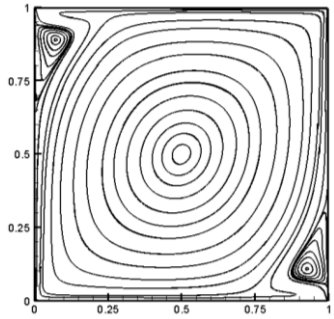

(c) *Re* = 1500

Figure 10: Streamline patterns of two-sided square cavity with antiparallel wall motion for different Reynolds numbers.

The increased Reynolds number results in the appearance of two secondary vortices near the top left and the bottom right corners of the lid-driven cavity and a very small shift of the primary vortex centre from the geometric centre of the cavity. It is also seen that, as the Reynolds number increases, the strength of the two secondary vortices near the top left and the bottom right corners of the cavity also increase in size. Figures 11 shows the comparisons of horizontal velocity profiles along vertical lines and vertical velocity profiles along horizontal lines passing through different points of the double-sided lid-driven square cavity (antiparallel wall motion) for the various Reynolds numbers and the agreement is excellent once again. It is seen that, the LBT-MRT model results given by all the figures and tables are in excellent agreement with those given by the FDM [1] and CE/SE Scheme [13]. This lends credibility to the present LBT-MRT model results for double-sided lid-driven square cavity with antiparallel wall motion problem.

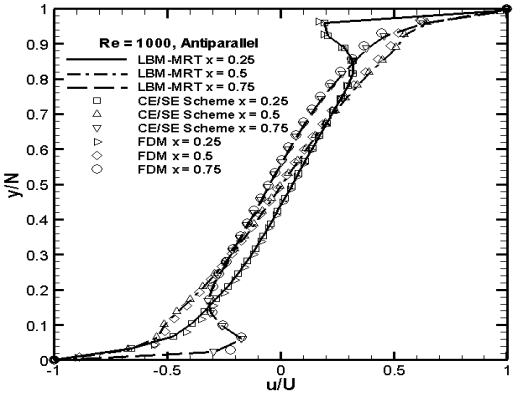

(a)

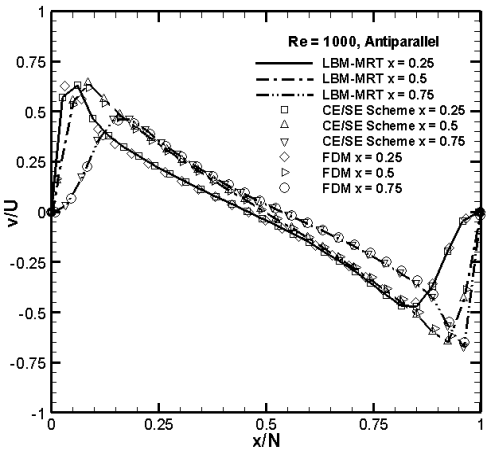

(b)

Figure 11: Antiparallel wall motion, *Re* = 1000: (a) horizontal velocity *u* along vertical lines (b) vertical velocity *v* along horizontal lines passing through *y* = 0.25, 0.50 and 0.75.

G. Aspect Ratio Effect

To study the aspect ratio effect, low to high aspect ratios of *K* = 0.25, 0.5, 2.0 and 5.0 is considered. Figures 12 (a), (b), (c) and (d) respectively show the streamline patterns of *Re* = 10 where the aspect ratios *K* = 0.25, 0.5, 2.0 and 5.0. From Figure 12, it is found that the flow structure inside the cavity changes considerably with the aspect ratio. Here, the near-wall primary vortices have the same sense of rotation and are well-separated as the aspect ratio is large. Figure 13 depicts the moderate Reynolds number of *Re* = 500 for different aspect ratios. Figure 14 depicts the high Reynolds number of *Re* = 1500 for different aspect ratios. It is seen that, as aspect ratio increases the vortices strength also increases.

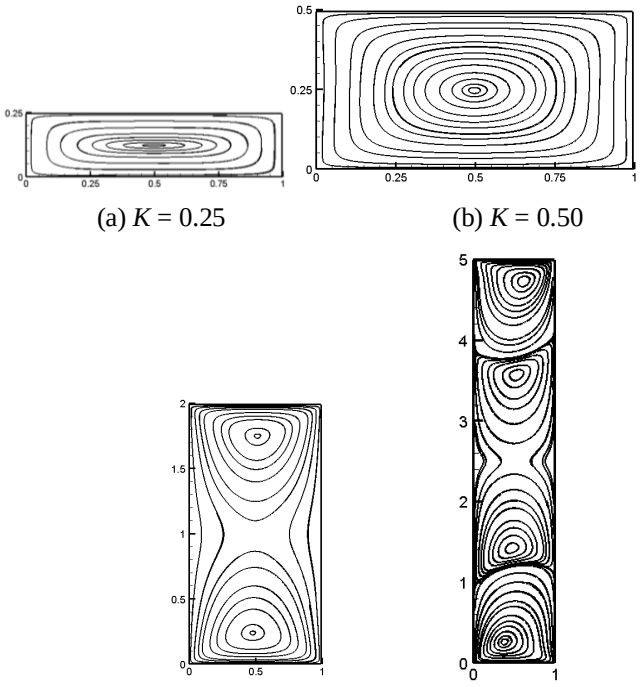

(a) $K = 0.25$ (b) $K = 0.50$

(c) $K = 2.0$ (d) $K = 5.0$

Figure 12: Streamline patterns of Re = 10 for two-sided antiparallel wall motion with different Aspect ratios (a) K = 0.25, (b) K = 0.50, (c) K = 1.0, (d) K = 2.0 and (e) K = 5.0.

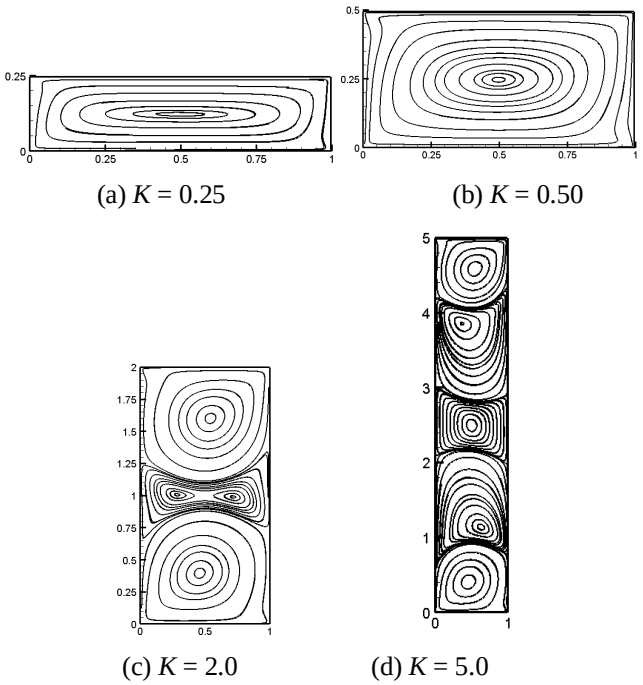

(a) $K = 0.25$ (b) $K = 0.50$

(c) $K = 2.0$ (d) $K = 5.0$

Figure 13: Streamline patterns of Re = 500 for two-sided antiparallel wall motion with different Aspect ratios (a) K = 0.25, (b) K = 0.50, (c) K = 1.0, (d) K = 2.0 and (e) K = 5.0.

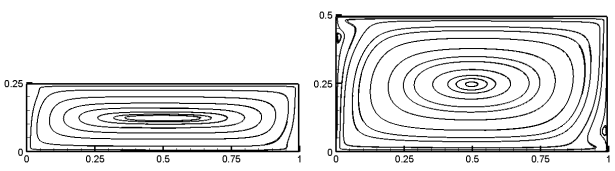

(a) $K = 0.25$ (b) $K = 0.50$

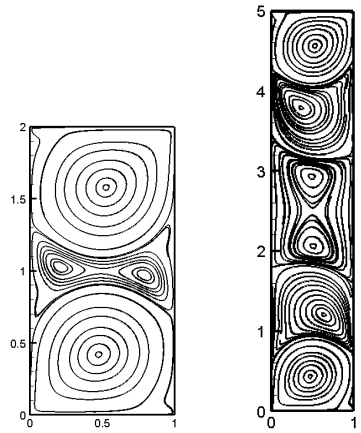

(c) $K = 2.0$ (d) $K = 5.0$

Figure 14: Streamline patterns of Re = 1500 for two-sided antiparallel wall motion with different Aspect ratios (a) K = 0.25, (b) K = 0.50, (c) K = 1.0, (d) K = 2.0 and (e) K = 5.0.

All of our computations are carried out on a Pentium 4-based PC with 512 MB RAM.

IV. CONCLUSION

In the present work, the flow in the two-sided lid-driven cavity for the parallel and antiparallel wall motion is numerically investigated using lattice Boltzmann technique with multi-relaxation-time (LBT-MRT) model. For the first geometry, namely, the single-sided lid-driven square cavity, some experimental, numerical and theoretical results exists, by reproducing which with the LBT-MRT model an insight about the appropriateness of the present boundary conditions was gained. This knowledge is then utilized when applying the LBT-MRT model to compute flows in the second geometry, namely, a two-sided lid-driven square cavity flows. The present computations not only confirms the flow features of the problem, but also reveals the effects of Reynolds number and the aspect ratio on the flow structure in the two-sided lid-driven deep cavity in a systematic way. Consequently these results, like those of the single lid-driven deep cavity flow, may be used for validating the algorithms for computing steady flows governed by the two-dimensional incompressible Navier-Stokes equations. To sum up, the present study reveals many interesting features of single-sided and two-sided lid-driven cavity flows and demonstrates the capability of the LBT-MRT model to capture these features.

REFERENCES

[1] D.A. Perumal, and A.K. Dass, "*Simulation of Incompressible flows in two-sided lid-driven square cavities – FDM",* CFD Letters, Vol. 2(1), pp. 13-24, 2010.

[2] D.A. Perumal, and A.K. Dass, "*Simulation of Incompressible flows in two-sided lid-driven square cavities – LBM",* CFD Letters, Vol. 2(1), pp. 25-38, 2010.

[3] D. Yu, R. Mei, L.S. Luo and W. Shyy, *"Viscous flow computations with the method of lattice Boltzmann equation",* Progress in Aerospace Sciences, Vol. 39, pp. 329-367, 2003.

[4] D.A. Perumal, and A.K. Dass., "*Application of Lattice Boltzmann Method for Incompressible viscous flows",* Applied Mathematical Modelling, Vol. 37(6), pp. 4075-4092, 2013.

[5] P.J. Dellar, "*Incompressible limits of Lattice Boltzmann equations using multiple relaxation times"*, Journal of Computational Physics, *Vol*. 190, pp. 351-370, 2003.

[6] R. Du, B. Shi, X. Chen, "*Multi-relaxation-time lattice Boltzmann model incompressible flow",* Physics Letters A, Vol. 359, pp. 564-572, 2006.

[7] P. Lallemand, and L.S. Luo, "*Theory of the lattice Boltzmann method: dispersion, dissipation, isotropy, Galilean invariance, and stability"*, Physical Review E, Vol. 61, pp. 6546-6562, 2000.

[8] D. d'Humieres, "*Generalized lattice Boltzmann equation, in rarefied gas dynamics: theory and simulations"*, Progress in Astronautics and Aeronautics, Edited by B.D. Shizgal and D.P. Weaver, AIAA, D.C. Washington, Vol. 159, pp. 450-458, 1992.

[9] P.N. Shankar, and M.D. Deshpande, "*Fluid mechanics in the driven cavity"*, Annual Review of Fluid Mechanics, Vol. 32, pp. 93-136, 2000.

[10] J.-S. Wu, and Y.-L. Shao, "*Simulation of lid-driven cavity flows by parallel lattice Boltzmann method using multi-relaxation-time scheme",* International Journal of Numerical Methods in Fluids, Vol. 46, pp. 921–937, 2004.

[11] D.A. Perumal, and A.K. Dass, "*Multiplicity of steady solutions in two-dimensional lid-driven cavity flows by lattice Boltzmann method",* Computers & Mathematics with Applications, Vol. 61(12), p. 3711-3721, 2011.

[12] U. Ghia, K.N. Ghia, C.T. Shin, "*High-Re solutions for incompressible flow using Naiver-Stokes equations and a multigrid method",* Journal of Computational Physics, Vol. 43, pp. 387-441, 1982.

[13] D-X. Yang and Zhang De-Liang, "*Applications of the CE/SE scheme to imcompressible flows in two-sided lid-driven square-cavities"*, Chinese Physics Letters, Vol. 29(8), p. 084717- 1-5, 2012.